Journal of Orthopaedic Research

Muscle optimization techniques impact the magnitude of calculated hip joint contact forces

Journal:	*Journal of Orthopaedic Research*
Manuscript ID:	JOR-13-0749.R3
Wiley - Manuscript type:	Research Article (Member)
Date Submitted by the Author:	n/a
Complete List of Authors:	Wesseling, Mariska; KU Leuven, Human Movement Biomechanics Research Group Derikx, Loes; KU Leuven, Human Movement Biomechanics Research Group; Radboud university medical center, Orthopaedic Research Laboratory de Groote, Friedl; KU Leuven, Department of Mechanical Engineering Bartels, Ward; KU Leuven, Department of Mechanical Engineering Meyer, Christophe; KU Leuven, University Hospital Pellenberg Verdonschot, Nico; Radboud university medical center, Orthopaedic Research Laboratory; University of Twente, Laboratory of Biomechanical Engineering Jonkers, Ilse; KU Leuven, Human Movement Biomechanics Research Group
Keywords:	Hip contact forces, Gait, Sit to stand, Static optimization, Optimization techniques

Muscle optimization techniques impact the magnitude of calculated hip joint contact forces

Mariska Wesseling[1], Loes C Derikx[1,2], Friedl de Groote[3], Ward Bartels[3], Christophe Meyer[4], Nico Verdonschot[2,5], Ilse Jonkers[1].

[1] Human Movement Biomechanics Research Group, KU Leuven, Leuven, Belgium

[2] Orthopaedic Research Laboratory, Radboud university medical center, Nijmegen, The Netherlands

[3] Department of Mechanical Engineering, KU Leuven, Leuven, Belgium

[4] University Hospital Pellenberg, KU Leuven, Belgium

[5] Laboratory of Biomechanical Engineering, University of Twente, Enschede, The Netherlands.

Running title: Muscle and hip contact forces

Corresponding author:

Mariska Wesseling

Human Movement Biomechanics Research Group

Katholieke Universiteit Leuven

Tervuursevest 101 - box 1501

3001 Leuven, Belgium

Tel.: +32 16 376463

Fax: +32 16 329197

mariska.wesseling@med.kuleuven.be

Abstract

In musculoskeletal modelling, several optimization techniques are used to calculate muscle forces, which strongly influence resultant hip contact forces (HCF). The goal of this study was to calculate muscle forces using four different optimization techniques, i.e. two different static optimization techniques, computed muscle control (CMC) and the physiological inverse approach (PIA). We investigated their subsequent effects on HCFs during gait and sit to stand and found that at the first peak in gait at 15-20% of the gait cycle, CMC calculated the highest HCFs (median 3.9 times peak GRF (pGRF)). When comparing calculated HCFs to experimental HCFs reported in literature, the former were up to 238% larger. Both static optimization techniques produced lower HCFs (median 3.0 and 3.1 pGRF), while PIA included muscle dynamics without an excessive increase in HCF (median 3.2 pGRF). The increased HCFs in CMC were potentially caused by higher muscle forces resulting from co-contraction of agonists and antagonists around the hip. Alternatively, these higher HCFs may be caused by the slightly poorer tracking of the net joint moment by the muscle moments calculated by CMC. We conclude that the use of different optimization techniques affects calculated HCFs, and static optimization approached experimental values best.

Keywords

Hip contact forces, gait, sit to stand, static optimization, optimization techniques.

Introduction

The hip contact force (HCF) is a relevant measure of joint loading. Changes in HCF have been related to osteoarthritis (OA) of the hip and knee[1,2]. However, experimental measurement of HCFs is not trivial and relies on the use of instrumented prostheses in hip arthroplasty patients[3,4]. Therefore, data collection is limited to a selected group of patients who underwent total hip surgery, resulting in a relatively small and specific dataset. Alternatively, musculoskeletal models in combination with dynamic simulations of motion have been used to calculate muscle forces and joint contact forces, so that larger populations comprising both healthy and diseased subjects can be studied.

The calculation of joint contact forces relies on the use of musculoskeletal models in combination with an optimization procedure to determine the muscle force distribution[5–8]. The resulting calculated joint forces have previously been validated using instrumented prostheses[3,6–8]. Most analyses use a static optimization (SO) technique to calculate muscle forces. SO uses an inverse dynamics approach: joint moments are used as a constraint to calculate individual muscle forces that satisfy the moment equilibrium at each time frame by minimizing muscle activation or muscle stress. As such, this method is a simplification of muscle physiology and does not account for muscle dynamics. Therefore, alternative methods were developed. Computed muscle control (CMC)[9] combines a forward integration of the dynamic equations with a static optimization to compute muscle excitations and muscle forces respectively, and therefore complies with time dependency of force production. Alternatively, the physiological inverse approach (PIA) includes muscle activation and contraction dynamics to calculate muscle forces and optimizes performance globally over time[10]. Several authors have compared the effect of different optimization techniques on calculated muscle activations[10–12] and compared them to experimentally measured electromyography (EMG) signals. Some have shown there is not much difference between static and dynamic

simulations[11]. Others show that PIA produces excitations and activations in closer agreement with the EMG signals[10,12].

However, the effect of specific muscle optimization techniques on calculated HCFs is not documented, while the optimization method and related boundary conditions used to calculate muscle forces can be assumed to strongly influence the calculated joint contact forces[13]. This effect of specific muscle optimization techniques on calculated HCFs is important to acknowledge when utilizing these forces as loading conditions in orthopaedic research applications, to study for example implant loading and bone adaptation[14–16]. Hence, the effect of the optimization technique on the output parameters is analysed, as this may influence such research applications. Therefore, the goal of this study was to quantify differences in 1) muscle forces and 2) the magnitude and orientation of the resultant HCFs when using four optimization techniques. Calculated HCFs were additionally compared against contact forces measured using instrumented prostheses (the HIP98 dataset[3]).

Methods

Movement analysis

Five healthy subjects (age 56±3 yrs., range 52-61 yrs.; BMI 22.3±1.59, range 20.6-24.0), 2 male and 3 female, were included in the study and signed informed consent. All subjects performed gait at self-selected speed (walking speed 1.28±0.13 m/s, range 1.1-1.4 m/s) as well as a sit to stand movement (sit to stand time 0.60±0.09 s, range 0.51-0.69 s) from an adjusted stool position imposing a 90° knee flexion angle. The sit to stand movement was defined from the moment of lift-off from the stool until the moment of minimal vertical ground reaction force after lift-off, i.e. just before standing upright[17]. A Plug-in-Gait marker set containing lower limb and trunk was used[18] including a three-marker cluster on both upper and lower legs and one additional marker on both medial knees and ankles during the static trials. Thus, a total of 40 markers were included. 3D marker trajectories were captured using

Vicon (100 Hz, VICON, Oxford Metrics, Oxford, UK) and force data was measured using two AMTI force platforms (1500 Hz, Advanced Mechanical Technology Inc., Watertown, MA).

Musculoskeletal Modelling

The Gait2392 musculoskeletal model installed with OpenSim[19] was used, which consists of 12 segments, 19 degrees of freedom and 92 musculotendon actuators. Simulations and analyses were performed in OpenSim 2.4.0[19]. To calculate HCFs, the model was first scaled based on the marker locations in a static pose. The scaled model was then used for an inverse kinematics procedure based on measured 3D marker trajectories to determine the kinematics of the movement. Subsequently, a residual reduction algorithm (RRA)[20] was applied, which minimizes the dynamic inconsistency between ground reaction forces and whole body kinematics introduced by errors in modelling and marker kinematics. This inconsistency is compensated by changing the kinematics and by adjusting the mass of the segments and the centre of mass of the torso. Since RRA is only applicable if ground reaction forces, exerted on both feet, are available, the gait cycle was restricted from toe off of the left leg until heel strike of the right leg.

To calculate muscle forces, four different methods were used. First, we used the static optimization procedure as provided in OpenSim (SO1)[11]. Muscle forces at each time instance of the movement are calculated while minimizing the instantaneous total squared muscle activation. A quadratic optimization criterion was adopted, since this has shown to produce the best agreement between EMG and muscle forces and reliably predict measured hip contact forces[21]. This method further includes muscle force-length-velocity relationships and reserve actuators that are activated whenever the total muscular moment is insufficient to balance the net joint moment. A second static optimization procedure (SO2) was developed in-house, based on Lenaerts et al.[5]. This optimization uses a cost function similar to SO1, but adds

constraints to the cost function to impose a physiological increase and decrease of muscle activation in time. In addition to the work of Lenaerts et al.[5], passive muscle forces were accounted for following the work of Rodrigo et al.[22]. Thirdly, we used CMC[9] which combines a static optimization with feedforward and feedback controls to calculate muscle excitations, and subsequent muscle forces. As this method is based on a forward simulation, the time dependency of the activation and contraction dynamics is explicitly accounted for. Fourthly, we applied the PIA[10], which globally optimizes squared muscle activations over the complete movement cycle while imposing muscle activation and contraction dynamics. The objective functions for all methods are provided in appendix A. The muscle forces were normalized to body weight and compared between the four methods. At the first and second peak, the magnitudes of the muscle forces were summed to indicate the total muscle load calculated by the optimization techniques.

Finally, for the four methods, HCFs of the right leg were calculated using the JointReaction analysis in OpenSim[23]. The time history of model-based HCFs as well as muscle activations and forces are provided in the supplementary material.

Validation of the muscle activations

During all trials, the EMG activity of the mm. tensor fasciae latae, rectus femoris, biceps femoris, medial hamstrings, gluteus maximus and the posterior, medial and anterior bundles of the m. gluteus medius were recorded using a wireless EMG system (Zero-wire EMG, Aurio, Milan, Italy). After appropriate skin cleaning, disposable surface electrodes (Pre-gelled Nutrode mini P10M0, 30 mm diameter, GE Medical Accessories Europe) were placed following the SENIAM guidelines[24] and based on manual palpation. EMG signals were band pass filtered (4th order, zero-lag Butterworth filter, cut-off-frequency between 20 and 400 Hz), rectified and then low pass filtered (4th order, zero-lag Butterworth filter, cut-off frequency of 10 Hz)[23]. All signals were normalized to their maximum in the gait cycle or sit to stand

movement. The muscle activations were calculated using the four optimization methods and compared to the measured EMG signals.

Validation of the hip joint contact forces

The calculated HCFs were evaluated against contact forces measured in four subjects (age 62±11 yrs., range 51-78 yrs.; BMI 29.0±2.65, range 26.2-32.6) with instrumented hip implants (HIP98)[3] during walking (walking speed 1.18±0.12 m/s, range 1.08-1.35 m/s) and rising from a chair (sit to stand time 0.81±0.03s, range 0.76-0.82s).

Data Analysis

For each of the four optimization methods the magnitude of the resultant HCFs were calculated per subject, both for gait and sit to stand. HCFs were normalized to body weight (BW) for comparison between optimization techniques. For comparing with HIP98, HCFs were normalized to the peak in ground reaction force (pGRF)[25] to better accommodate for differences in gait dynamics between subjects. The contact forces were subsequently averaged over the subjects by calculating 'typical signals'[26]. This was done for the minimum, maximum, 25th and 75th percentile, median and average of the normalized resultant forces of the five subjects, respectively. Similarly, typical signals were calculated for the HCFs measured in the four HIP98 subjects.

During normal gait, the HCF measured in instrumented prostheses shows two peaks, i.e. at 15-20% of gait cycle (first peak) and at 45-55% of gait cycle (second peak). Muscle forces were compared between optimization techniques at these two peaks in gait and at the peak in sit to stand. Subsequently, the difference between HIP98 and the calculated HCFs at these peaks was determined. Furthermore, the 3D orientation of the HCF was averaged over subjects and compared with the orientation of the typical signal in the HIP98 dataset.

Results

Hip contact forces

For gait trials, the CMC contact forces were highest throughout the entire gait cycle (Figure 1A). The other optimization techniques resulted in rather similar HCF patterns, especially during stance phase. During swing phase, a more distinct difference was seen with the lowest average HCF for SO1 (Figure 1A). At the first peak, the contact forces calculated using CMC was highest (median of 3.9 pGRF), while both static optimizations were closest to HIP98 forces (median of 3.0 and 3.1 pGRF for SO1 and SO2, respectively; Figure 2A). The PIA calculated contact forces close to SO1 and SO2 (median of 3.2 pGRF). At the second peak (Figure 2B), again HCFs were highest when using CMC (median of 5.6 pGRF). All optimization techniques tended to overestimate the HCF compared to the measured forces (Figure 1B, Table 1).

The 3D orientation angles of the calculated HCFs were very similar, but they differed from the HCF described in HIP98. At both peaks in the gait cycle, calculated HCFs generally resulted in a more anterior and medial loading compared to the HIP98 data (Figure 3 A and B).

For sit to stand trials, the use of CMC induced the largest HCF (Figure 4A, Table 1). When using both SO techniques, peak contact forces, just after lift-off, were closest to the measured HIP98 data (median of 4.7 and 5.3 pGRF for SO1 and SO2, respectively; Figure 5). HCFs resulting from PIA were only slightly lower than for CMC at the peak (median of 5.6 and 5.9 pGRF respectively), but were closer to measured data in the second part of the movement (Figure 4B). The calculated orientation angles showed that HCFs presented a more anterior and lateral loading than in HIP98 (Figure 3C). The use of PIA resulted in an orientation angle that was most comparable to HIP98.

Muscle forces

The sum of the magnitudes of the muscle forces calculated by CMC was higher than for other optimization techniques at both HCF peaks during walking and at the HCF peak during sit to

stand (Figure 6). Muscle forces calculated by PIA are slightly lower during gait and more comparable to SO1 and SO2 in sit to stand. At the second peak in gait the total muscle force found for CMC was up to 22% larger compared to SO2. Specifically, the force calculated for the bundles of the gluteus maximus (first peak) and medius (second peak) were higher for CMC.

Appendix B shows the results of a qualitative comparison between the average normalized EMG activation patterns and the average muscle activation patterns calculated using the different optimization techniques.

Discussion

This study compared muscle forces and the subsequent HCFs calculated using four different optimization techniques. CMC calculated the largest sum of muscle forces for both gait and sit to stand while particularly SO2 calculated lower forces (Figure 6). The same trend was seen in the calculation of the HCFs; both static optimization techniques showed the lowest HCFs. The additional constraints to include a physiological increase and decrease of muscle activation in time and the inclusion of passive muscle forces (SO2) did not majorly affect the HCFs compared to a standard SO formulation (SO1, Figure 1A). In contrast, HCFs increased drastically when using CMC (Figure 1A). The agreement in HCF between SO techniques and PIA shows that the activation and contraction dynamics can be integrated without inducing an excessive overestimation of the HCFs as observed by CMC.

There may be two causes for the increased muscle force production found for CMC relative to other optimization techniques. First, the higher muscle forces may reflect co-contraction of agonists and antagonists to satisfy the 3D joint moments around the hip, which may explain the increased HCFs found for this method. More specifically, a post-hoc analysis of the muscle moments of the primary muscles acting around the hip joint confirmed these co-contractions, particularly at the second peak in gait (Figure 7B). At this time instant, an

internal hip abduction and flexion moment is present. The recruitment of the bundles of the gluteus medius muscle induces this hip abduction moment, but also produces a hip extension moment. Therefore additional contraction of the mm. iliacus and psoas is induced to deliver the required hip flexion moment. Although this co-contraction is seen in all optimization techniques, for both peaks in gait (Figure 7A and B) and sit to stand (Figure 7C), the effect is largest for CMC. This may be explained by the fact that passive muscle forces and muscle dynamics are accounted for. More specifically, muscle forces cannot change instantaneously due to activation and contraction dynamics and hence force build-up in the agonists will coincide with force build-off in the antagonists.

The second possible cause for the increased muscle and contact force found by CMC could be the fact that this implementation allows for calculating a muscle generated moment that deviates slightly more from the moment necessary to counteract the net joint moments. This results in a larger difference between the muscle generated moments and net joint moments, mainly in the frontal and sagittal planes (Figure 8). Although defined in different manners, all optimization techniques allow for a deviation from the net joint moment. Largest deviations were found for CMC, mainly for abduction. This might be explained by the feedforward and feedback controls imposed by CMC for tracking the kinematics combined with the physiological constraints on muscle force rise and decay which cause increased muscle generated moments around the hip.

HCFs calculated using CMC deviated most from other optimization techniques, especially during gait trials (Figure 1B). Since the input (musculoskeletal model, kinematics and ground reaction forces) was identical for all of the optimization procedures, the differences in the resulting HCFs must be attributed to the different optimization techniques. However, all techniques systematically overestimated the magnitude of the HCFs as compared to those measured using instrumented prostheses[3]. In addition to overestimated magnitudes, the

calculated contact forces showed a more out of plane loading of the hip joint in the frontal plane, i.e. a more anterior loading (Figure 3). These differences with the HIP98 data may have arisen from modelling choices that were made before the optimization step, since there are many parameters in musculoskeletal models, e.g. attachment points, number of muscles in the model and muscle parameters, that affect the estimated muscle forces and the consequential effect on the HCF. Hence, further research is warranted to unravel the complexity of these issues to obtain more robust and reliable musculoskeletal predictions.

Additional contraction was seen in all optimization techniques, for both peaks in gait and sit to stand, which may partly explain the overestimation on HIP98. The optimization procedures solve the redundancy problem by minimizing the total of the squared muscle activations after the joint moment equilibrium at the hip and other joints of the lower limb have been satisfied. The resulting co-activations will contribute to the overestimation of the contact forces[27]. Specifically at the second peak in gait, large opposing moments are found in the sagittal and transversal planes (Figure 7B). At the first peak in gait, only mm. rectus femoris and tensor fasciae latae opposed the required extension moment (Figure 7A) which may explain why HCF overestimations were lower at this time instance. Also for sit to stand overestimations of HCFs were lower compared to the first peak in gait, as none of the recruited muscles opposed the external flexion moment (Figure 7C).

The overestimation of joint contact forces has been described before. Klein Horsman[28] compared one young and healthy subject with the HIP98 data, using inverse forward dynamic optimization[29] and an energy related criterion[30] and found that the second peak was 200% larger than the measured HCF. Although a different muscle optimization technique was used, the magnitude of the second peak was also much larger than the first peak, and comparable to the present study. Moreover, Mellon et al.[31] found contact forces up to 229% larger than those

found by Bergmann et al.[3], although this difference was not statistically significant. For sit to stand more comparable results were found.

In contrast, several other studies showed HCFs that are closer to HIP98 data than those reported in the current study[6–8,25], which may be attributed to different modelling choices. First of all, these simulations were based on the subjects from the HIP98 dataset[6–8] and therefore differences between healthy subjects and the HIP98 patients were not applicable. Furthermore, Stansfield et al.[8] used a static optimization which included a minimization of the contact forces. This additional criterion redistributes muscle forces to synergists without increasing the HCF. Heller et al.[6] used a linear optimization that minimized the sum of muscle forces and limited the maximal muscle force. Furthermore, others showed that the number of muscles and lines of action in the musculoskeletal model affect the HCF[7]. Besides that, several studies included subject-specific information in their models. Martelli et al.[25] included a subject that was body-matched to the cadaver from which a subject-specific model was created. Alternatively, CT images have been used to further personalize the model[8,31]. Comparing these studies to the results in the current work show that musculoskeletal modelling involves many steps starting from kinematic and kinetic measurements, the choice of a musculoskeletal model, adapting that model to the subject-specific anatomy and the choice of an optimization criterion. All these steps have a major effect on the end results, however, in this study we only focussed on the potential effects of the choice of optimization technique.

When interpreting the results of this study, a number of limitations should be taken into account. The calculated muscle activations compared only moderately to experimental EMG for both gait and sit to stand (appendix B), which has been reported in previous research as well[10–12]. However, since only very few muscles around the hip can be appropriately

measured using surface EMG, the comparison of activation to EMG signals can only partially reflect the effect of the optimization techniques.

As a second limitation, we used experimental data from healthy subjects to calculate HCFs and compared these to an average HCF measured in four patients with instrumented prostheses. Consequently, observed differences between measured and calculated HCFs may partially result from subject characteristics. First, gait speeds in our population of control subjects were higher than in the normal walking trials in HIP98 (1.28 m/s vs. 1.18 m/s), which can lead to increased contact forces[3]. Second, hip moments were generally lower in the HIP98 patients than in our healthy control subjects, mainly around 50% of the gait cycle (in hip flexion 3.5 vs. 6.7 %BW*m and in hip adduction 6.5 vs. 7.2 %BW*m). These higher external moments determine the muscle forces that need to be produced to satisfy the moment equilibrium and therefore influence the HCF. A fairer comparison would have been to calculate the HCFs using the experimental data made available via Orthoload[32] and compare them with their measured HCFs. However, the restricted number of experimental markers made the calculation of the joint angles highly sensitive to the marker definition in the model, which could only be partially reproduced based on the available documentation.

In conclusion, this study showed that the calculation of hip contact forces was sensitive to the optimization method used to calculated muscle forces. Both SO techniques produced results closest to measured HCFs, while CMC calculated the highest HCFs. PIA showed that activation and contraction dynamics can be included in the optimization without excessively increasing contact forces. However, other modelling choices had a distinct effect on the calculated loads as well, although identification of these factors was not within the scope of this study. Further research is therefore required to assess the effects of other modelling steps to come to a valid and robust prediction of muscle and joint contact forces in the lower limb.

Acknowledgments

This work was funded by the Agency for Innovation by Science and Technology (IWT-TBM no 100786), Fonds NutsOhra and the Dutch Cancer Foundation.

References

1. Lenaerts G, Mulier M, Spaepen A, et al. 2009. Aberrant pelvis and hip kinematics impair hip loading before and after total hip replacement. Gait & posture 30(3): 296–302.

2. Felson DT. 2004. Obesity and Vocational and Avocational Overload of the Joint as Risk Factors for Osteoarthritis. The journal of rheumatology 31(S70): 2–5.

3. Bergmann G, Deuretzbacher G, Heller M, et al. 2001. Hip contact forces and gait patterns from routine activities. Journal of biomechanics 34(7): 859–871.

4. Bergmann G, Graichen F, Rohlmann A. 1993. Hip joint loading during walking and running, measured in two patients. Journal of biomechanics 26(8): 969–990.

5. Lenaerts G, De Groote F, Demeulenaere B, et al 2008 Subject-specific hip geometry affects predicted hip joint contact forces during gait. Journal of biomechanics 41(6):1243–1252.

6. Heller MO, Bergmann G, Deuretzbacher G, et al. 2001 Musculo-skeletal loading conditions at the hip during walking and stair climbing. Journal of biomechanics 34(7):883–893.

7. Modenese L, Phillips ATM. 2012. Prediction of hip contact forces and muscle activations during walking at different speeds. Multibody system dynamics 28:157–168.

8. Stansfield BW, Nicol AC, Paul JP, et al. 2003. Direct comparison of calculated hip joint contact forces with those measured using instrumented implants. An evaluation of a three-dimensional mathematical model of the lower limb. Journal of biomechanics 36(7):929–936.

9. Thelen DG, Anderson FC, Delp SL. 2003. Generating dynamic simulations of movement using computed muscle control. Journal of biomechanics 36(3): 321–328.

10. De Groote F, Pipeleers G, Jonkers I, et al. 2009. A physiology based inverse dynamic analysis of human gait: potential and perspectives. Computer methods in biomechanics and biomedical engineering 12(5):563–574.

11. Anderson FC, Pandy MG. 2001. Static and dynamic optimization solutions for gait are practically equivalent. Journal of biomechanics 34(2):153–161.

12. De Groote F, Demeulenaere B, Swevers J, et al. 2012. A physiology-based inverse dynamic analysis of human gait using sequential convex programming: a comparative study. Computer methods in biomechanics and biomedical engineering 15(10):1093–1102.

13. Correa T, Crossley KM, Kim HJ, Pandy MG. 2010. Contributions of individual muscles to hip joint contact force in normal walking. Journal of biomechanics 43(8):1618–1622.

14. Pankaj P. 2013. Patient-specific modelling of bone and bone-implant systems: the challenges. Int. journal for numerical methods in biomedical engineering 29:233–249.

15. Speirs AD, Heller MO, Duda GN, Taylor WR. 2007. Physiologically based boundary conditions in finite element modelling. Journal of biomechanics. 40(10): 2318–2323.

16. van der Ploeg B, Tarala M, Homminga J, et al. 2012. Toward a more realistic prediction of peri-prosthetic micromotions. Journal of orthopaedic research 30(7): 1147–1154.

17. McGibbon CA, Goldvasser D, Krebs DE, Moxley Scarborough DM. 2004. Instant of chair-rise lift-off can be predicted by foot-floor reaction forces. Human movement science 23(2):121–132.

18. Davis RB, Ounpuu S, Tyburski D, Gage JR. 1991. A gait analysis data collection and reduction technique. Hum. Mov. Sci. 10:575–587.

19. Delp SL, Anderson FC, Arnold AS, et al. 2007. OpenSim: open-source software to create and analyze dynamic simulations of movement. IEEE transactions on bio-medical engineering 54(11): 1940–1950.

20. Thelen DG, Anderson FC. 2006. Using computed muscle control to generate forward dynamic simulations of human walking from experimental data. Journal of biomechanics 39(6):1107–1115.

21. Modenese L, Phillips ATM, Bull AMJ. 2011. An open source lower limb model: Hip joint validation. Journal of biomechanics 44(12):2185–2193.

22. Rodrigo SE, Ambrósio JAC, Tavares da Silva MP, Penisi OH. 2008. Analysis of Human Gait Based on Multibody Formulations and Optimization Tools. Mechanics based design of Structures and Machines 36(4):446–477.

23. Steele KM, Demers MS, Schwartz MH, Delp SL. 2012. Compressive tibiofemoral force during crouch gait. Gait & posture 35(4): 556–560.

24. Hermens HJ, Freriks B, Disselhorst-Klug C, Rau G. 2000. Development of recommendations for SEMG sensors and sensor placement procedures. Journal of electromyography and kinesiology. 10(5): 361–374.

25. Martelli S, Taddei F, Cappello A, et al. 2011. Effect of sub-optimal neuromotor control on the hip joint load during level walking. Journal of biomechanics 44(9):1716–1721.

26. Bender A, Bergmann G. 2012. Determination of typical patterns from strongly varying signals. Computer methods in biomechanics and biomedical engineering 15(7): 761–769.

27. Pedersen D, Brand R, Cheng C, Arora J. 1987. Direct comparison of muscle force predictions using linear and nonlinear programming. Journal of biomechanical engeneering 109:192–199.

28. Klein Horsman MD. 2007. The Twente Lower Extremity Model: Consistent Dynamic Simulation of the Human Locomotor Apparatus. Enschede: Gildeprint Drukkerijen; p 82-97.

29. Van Der Kooij H, Van Der Helm FC. 2003. Human gait analysis application of a new inverse/forward dynamic optimization (IFDO) method to solve the load sharing problem. In: International symposium on computer simulation in biomechanics. Sydney.

30. Praagman M, Chadwick EKJ, van der Helm FCT, Veeger HEJ. 2006. The relationship between two different mechanical cost functions and muscle oxygen consumption. Journal of Biomechanics 39(4):758–765.

31. Mellon SJ, Grammatopoulos G, Andersen MS, et al. 2013. Individual motion patterns during gait and sit-to-stand contribute to edge-loading risk in metal-on-metal hip resurfacing. Journal of engeneering in medicine 227(7):799–810.

32. Bergmann G (ed). Charité Universitaetsmedizin Berlin. Orthoload. 2008. Accessed March 13 2012 from http://www.OrthoLoad.com.

Tables

Table 1. The range of differences between calculated HCF and HIP98 [%] among subjects at the first and second peak in gait and at the peak during sit to stand. HCFs were calculated using different optimization techniques and normalized to the peak in ground reaction force (pGRF) to account for the differences in gait dynamics between subjects.

		SO1	SO2	CMC	PIA
Gait	Difference with HIP98 at the first peak [%]	4.5-56	3.6-47	46-88	12-69
	Difference with HIP98 at the second peak [%]	56-162	62-139	120-238	72-187
Sit to stand	Difference with HIP98 at the peak [%]	20-67	32-76	34-127	38-118

Figure Legends

Figure 1. A) Average hip contact forces (normalized to body weight (BW)) over the five subjects for gait calculated using different optimization techniques, shown from toe off of the left leg until heel strike of the right leg. Two peaks were defined, i.e. the first (at 15-20% of gait cycle) and second peak (at 45-55% of gait cycle). B) Calculated hip contact forces compared with experimental hip contact forces from HIP98. HCFs were normalized to the

peak in ground reaction force (pGRF) to account for the differences in gait dynamics between subjects.

Figure 2. Distribution of hip contact force (normalized to the peak in ground reaction force (pGRF)) among subjects at the first (A) and second peak (B) during a gait cycle using different optimization techniques. The minimum, 25th percentile, median, 75th percentile and maximum values are shown.

Figure 3. Direction of hip contact force (HCF) in the frontal and transverse planes calculated using different optimization techniques and measured *in vivo* (HIP98), at the first (A) and second peak (B) during gait and at the peak HCF during sit to stand (C). The force vectors of the different optimization techniques have a similar direction and are therefore difficult to distinguish.

Figure 4. A) Average hip contact forces (normalized to body weight (BW)) over the five subjects for sit to stand calculated using different optimization techniques. B) Calculated hip contact forces compared with experimental hip contact forces from HIP98. HCFs were normalized to the peak in ground reaction force (pGRF) to account for the differences in motion dynamics between subjects.

Figure 5. Distribution of hip contact force (normalized to the peak in ground reaction force (pGRF)) among subjects at the peak in sit to stand using different optimization techniques. The minimum, 25th percentile, median, 75th percentile and maximum values are shown.

Figure 6. Calculated muscle forces and sum of the muscle forces (SUM MF) for the different optimization techniques for the first and second peak in gait (A and B respectively) and peak in sit to stand (C). The most active muscles spanning the hip joint are shown. The force delivered by other muscles is generally lower than 1N.

Figure 7. Contribution of muscles to the hip moments at the first (A) and second (B) peak during gait and the peak in sit to stand (C). NJM is the net the joint moment calculated using

an inverse dynamics procedure, MMCON and MMOP are respectively the sum of muscle moments contributing to and opposing the net joint moment. Note the different scales on the vertical axes.

Figure 8. Net joint moment (NJM) and the difference between absolute muscle generated moment and net joint moment for the different optimization techniques, e.g. the deviation from the net joint moment. When the net joint moment is satisfied by the optimization, the muscle moment and joint moment will be equal, i.e. the difference between muscle moment and net joint moment is zero.

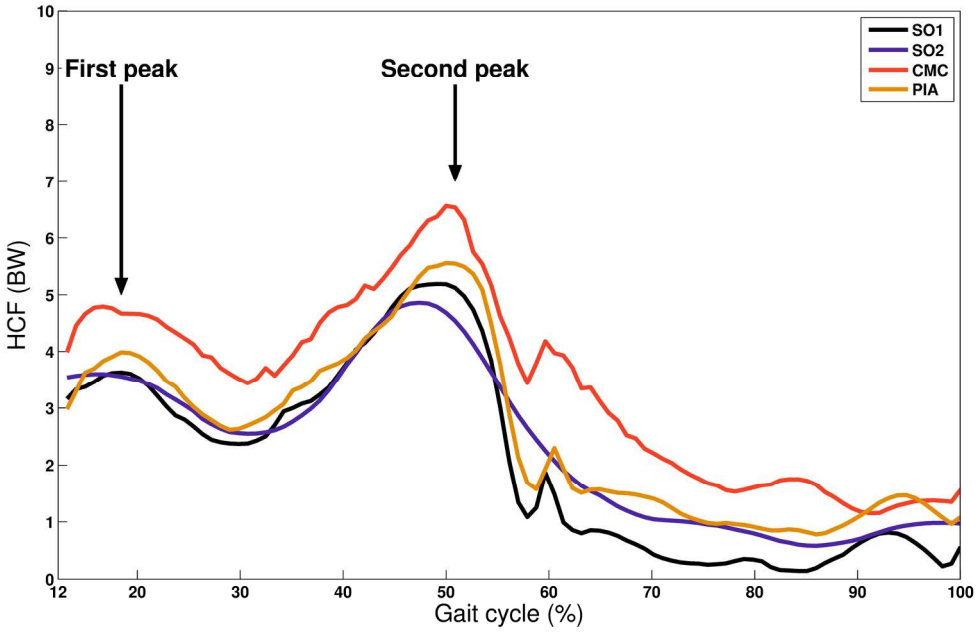

Figure 1. A) Average hip contact forces (normalized to body weight (BW)) over the five subjects for gait calculated using different optimization techniques, shown from toe off of the left leg until heel strike of the right leg. Two peaks were defined, i.e. the first (at 15-20% of gait cycle) and second peak (at 45-55% of gait cycle).
187x133mm (300 x 300 DPI)

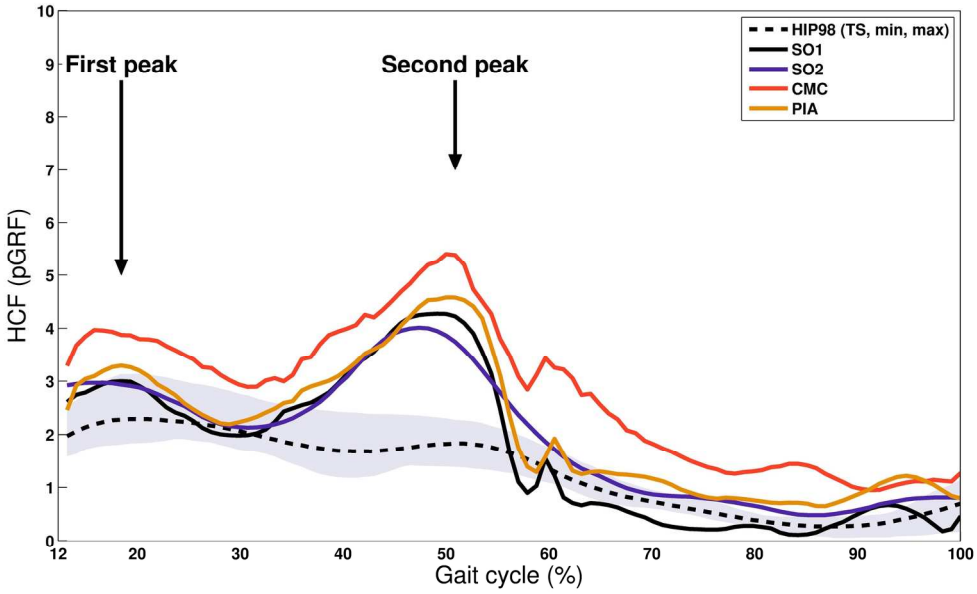

Figure 1. B) Calculated hip contact forces compared with experimental hip contact forces from HIP98. HCFs were normalized to the peak in ground reaction force (pGRF) to account for the differences in gait dynamics between subjects.
176x116mm (300 x 300 DPI)

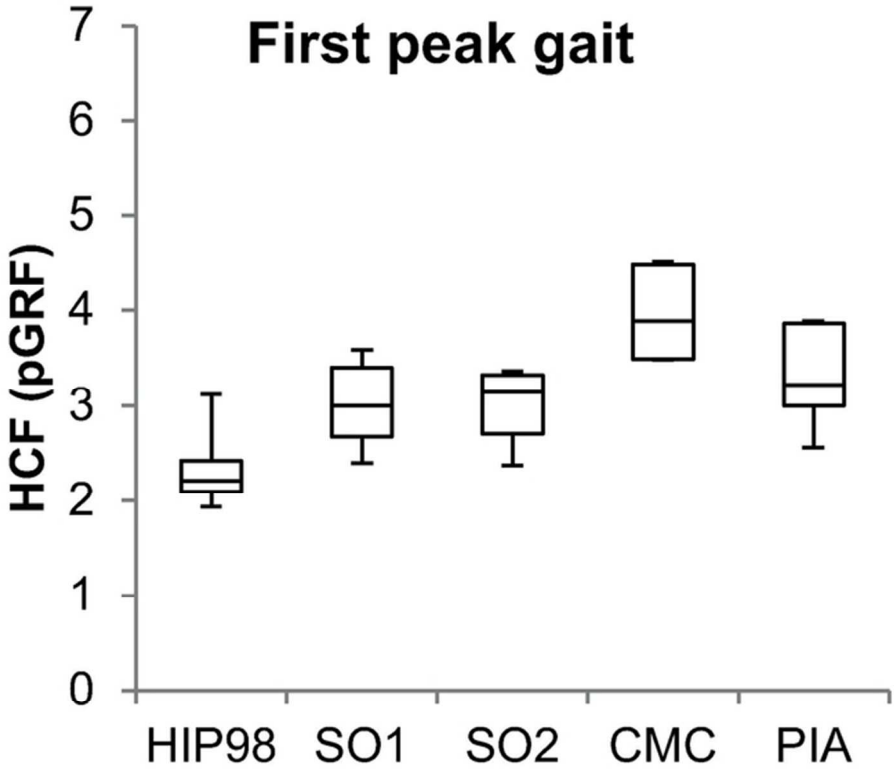

Figure 2A. Distribution of hip contact force (normalized to the peak in ground reaction force (pGRF)) among subjects at the first peak during a gait cycle using different optimization techniques.
61x51mm (300 x 300 DPI)

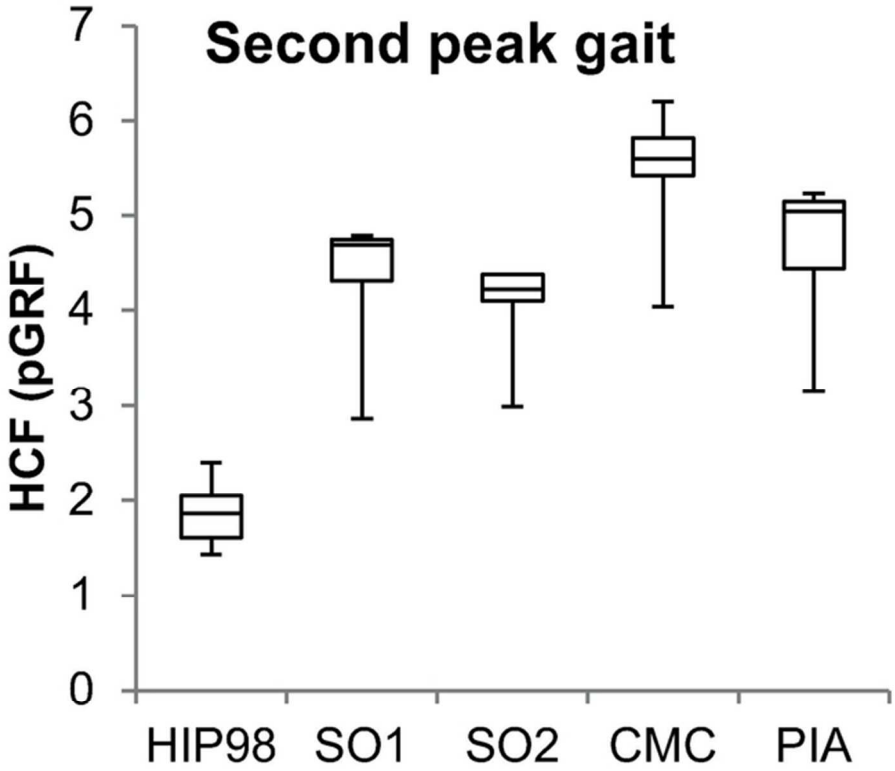

Figure 2B. Distribution of hip contact force (normalized to the peak in ground reaction force (pGRF)) among subjects at the second peak during a gait cycle using different optimization techniques.
61x51mm (300 x 300 DPI)

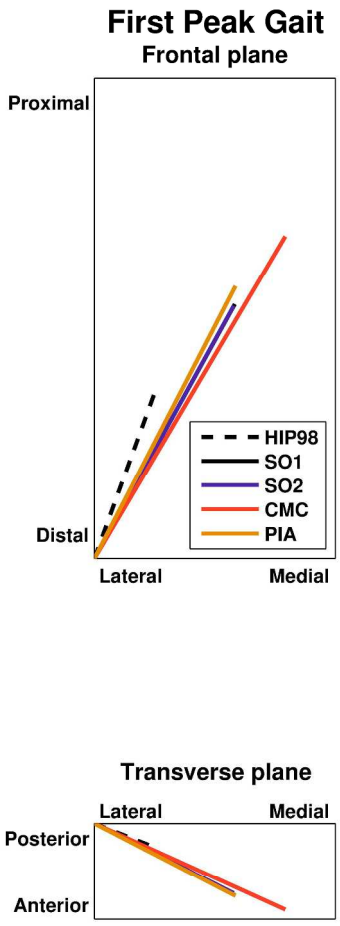

Figure 3A. Direction of hip contact force (HCF) in the frontal and transverse planes calculated using different optimization techniques and measured in vivo, at the first peak during gait. The force vectors of the different optimization techniques have a similar direction and are therefore difficult to distinguish.
218x546mm (300 x 300 DPI)

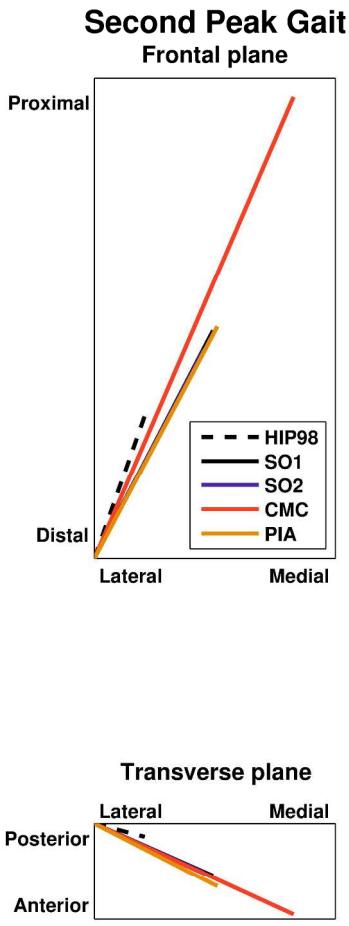

Figure 3B. Direction of hip contact force (HCF) in the frontal and transverse planes calculated using different optimization techniques and measured in vivo, at the second peak during gait. The force vectors of the different optimization techniques have a similar direction and are therefore difficult to distinguish.
218x546mm (300 x 300 DPI)

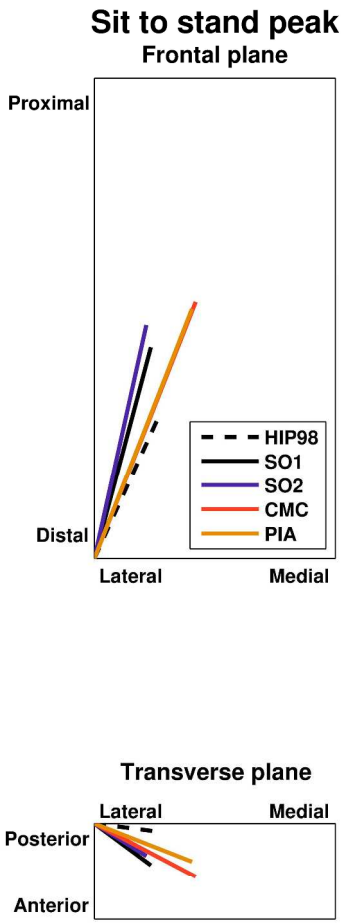

Figure 3C. Direction of hip contact force (HCF) in the frontal and transverse planes calculated using different optimization techniques and measured in vivo, at the peak HCF during sit to stand. The force vectors of the different optimization techniques have a similar direction and are therefore difficult to distinguish.
218x546mm (300 x 300 DPI)

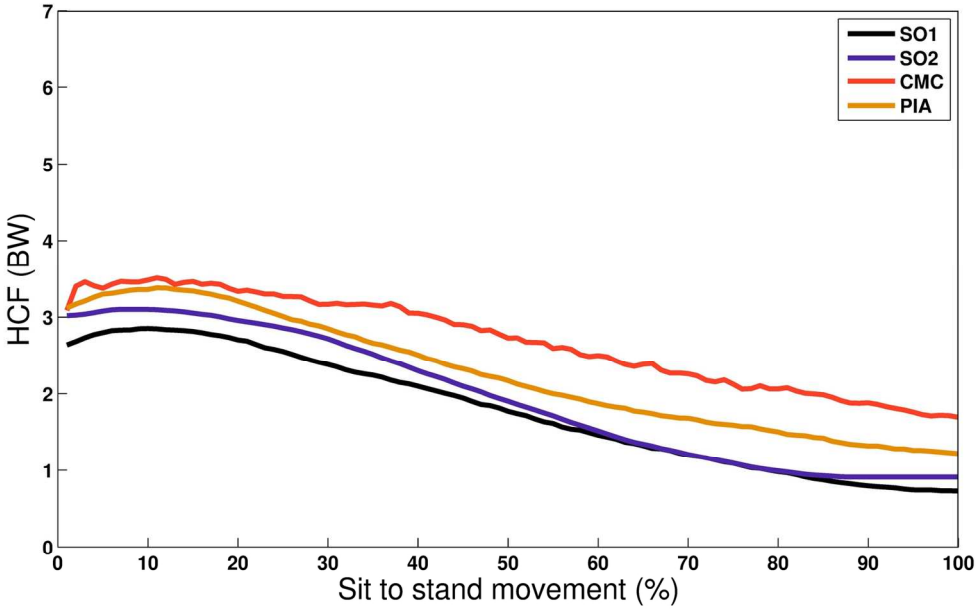

Figure 4. A) Average hip contact forces (normalized to body weight (BW)) over the five subjects for sit to stand calculated using different optimization techniques.
146x98mm (300 x 300 DPI)

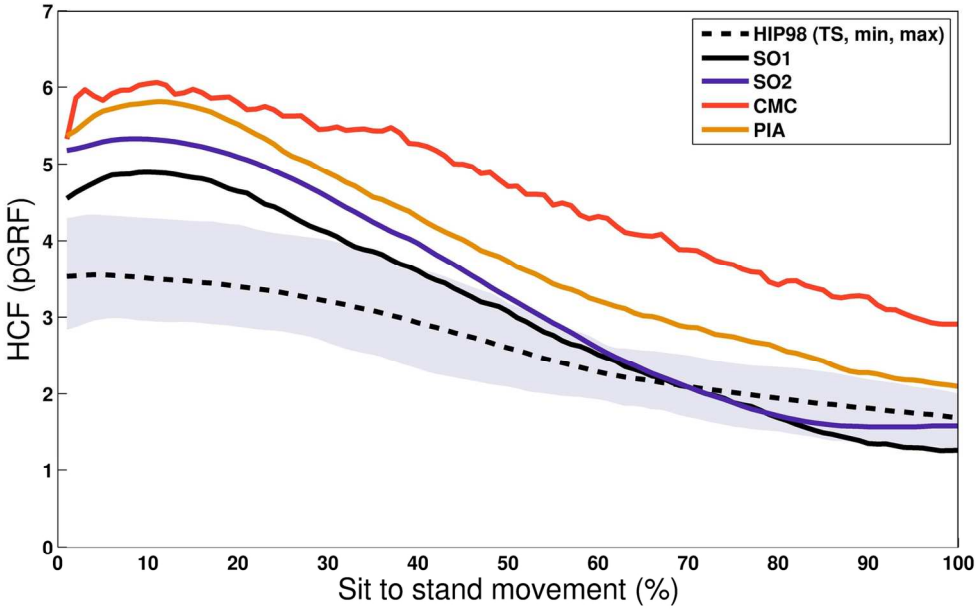

Figure 4. B) Calculated hip contact forces compared with experimental hip contact forces from HIP98. HCFs were normalized to the peak in ground reaction force (pGRF) to account for the differences in motion dynamics between subjects.
146x98mm (300 x 300 DPI)

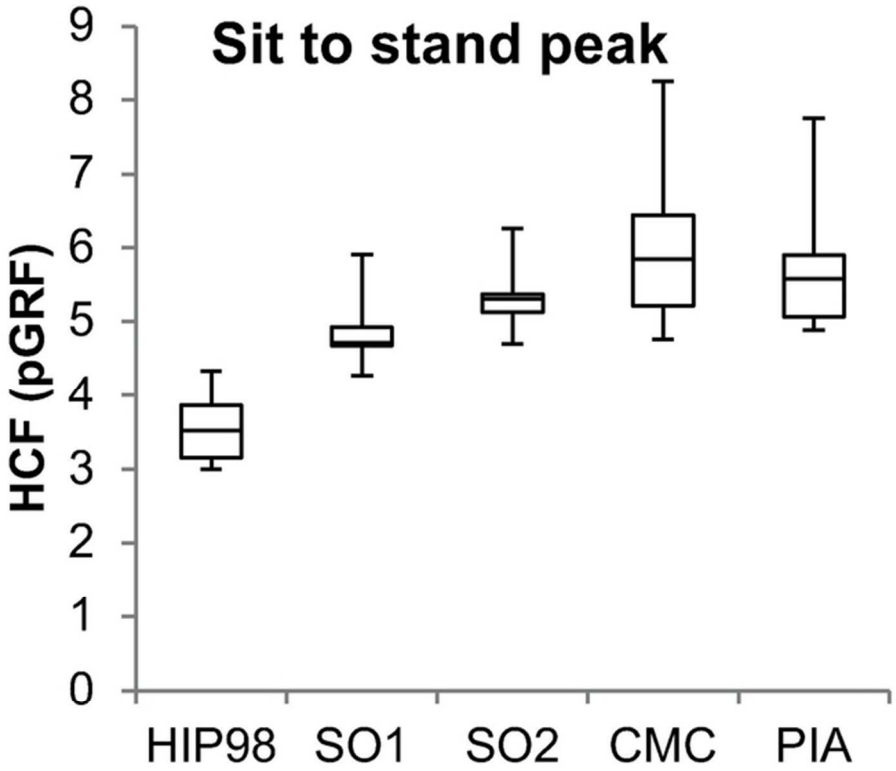

Figure 5. Distribution of hip contact force (normalized to the peak in ground reaction force (pGRF)) among subjects at the peak in sit to stand using different optimization techniques.
61x51mm (300 x 300 DPI)

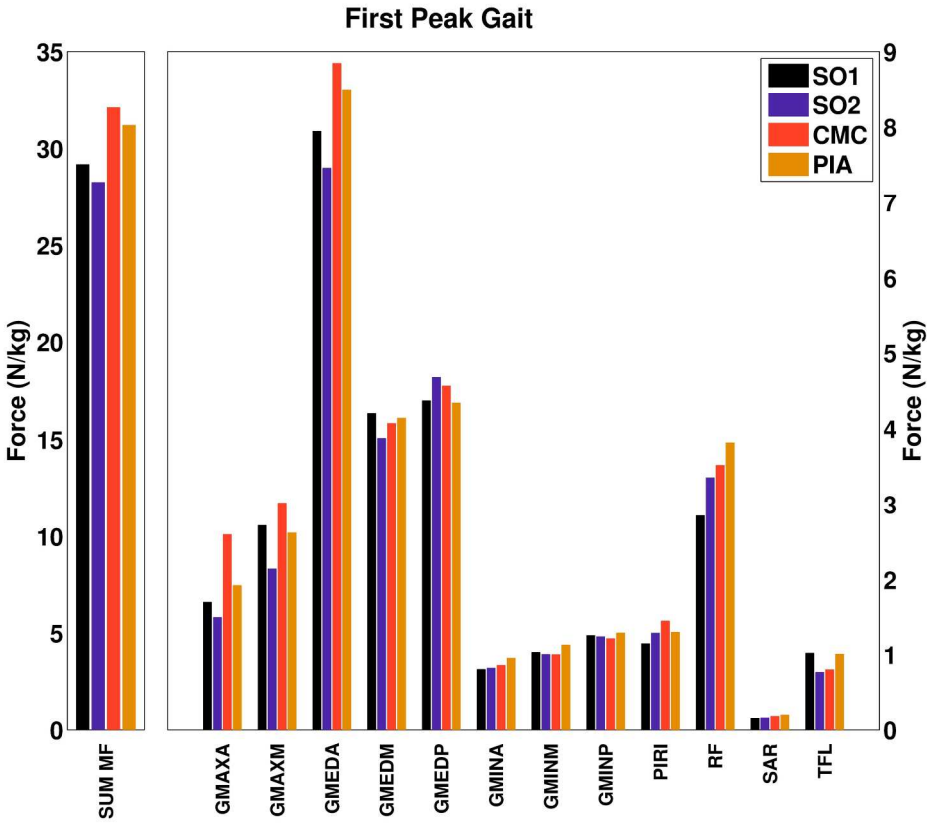

Figure 6A. Calculated muscle forces and sum of the muscle forces (SUM MF) for the different optimization techniques for the first peak in gait. The most active muscles spanning the hip joint are shown. The force delivered by other muscles is generally lower than 1N.
218x182mm (300 x 300 DPI)

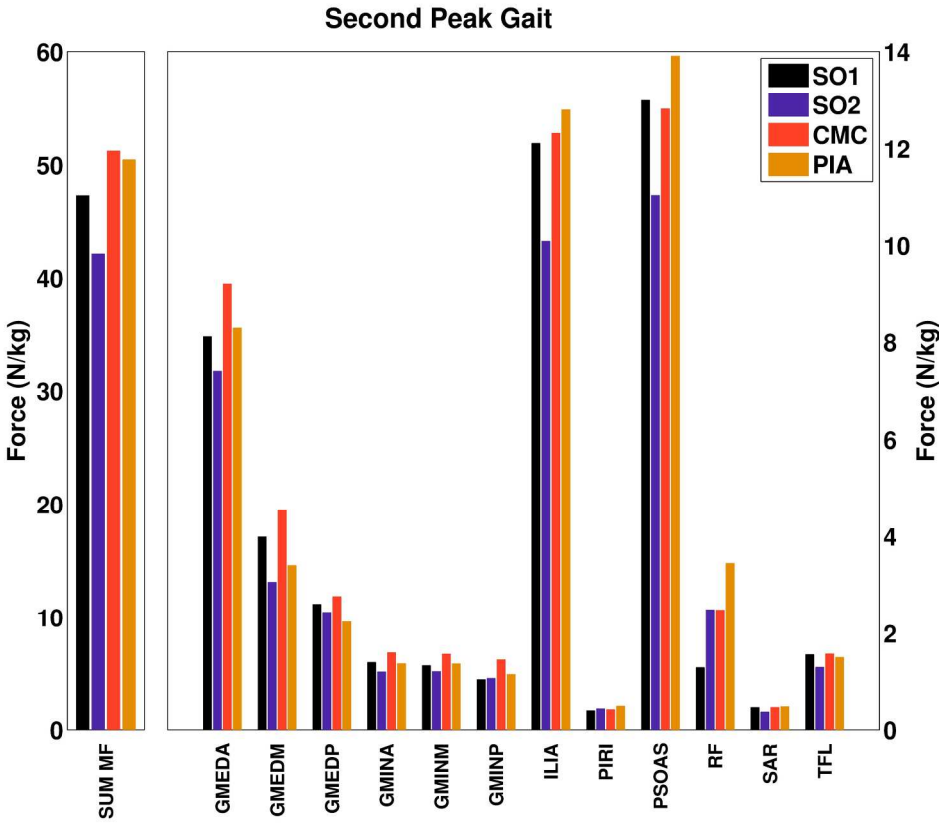

Figure 6B. Calculated muscle forces and sum of the muscle forces (SUM MF) for the different optimization techniques for the second peak in gait. The most active muscles spanning the hip joint are shown. The force delivered by other muscles is generally lower than 1N.
218x182mm (300 x 300 DPI)

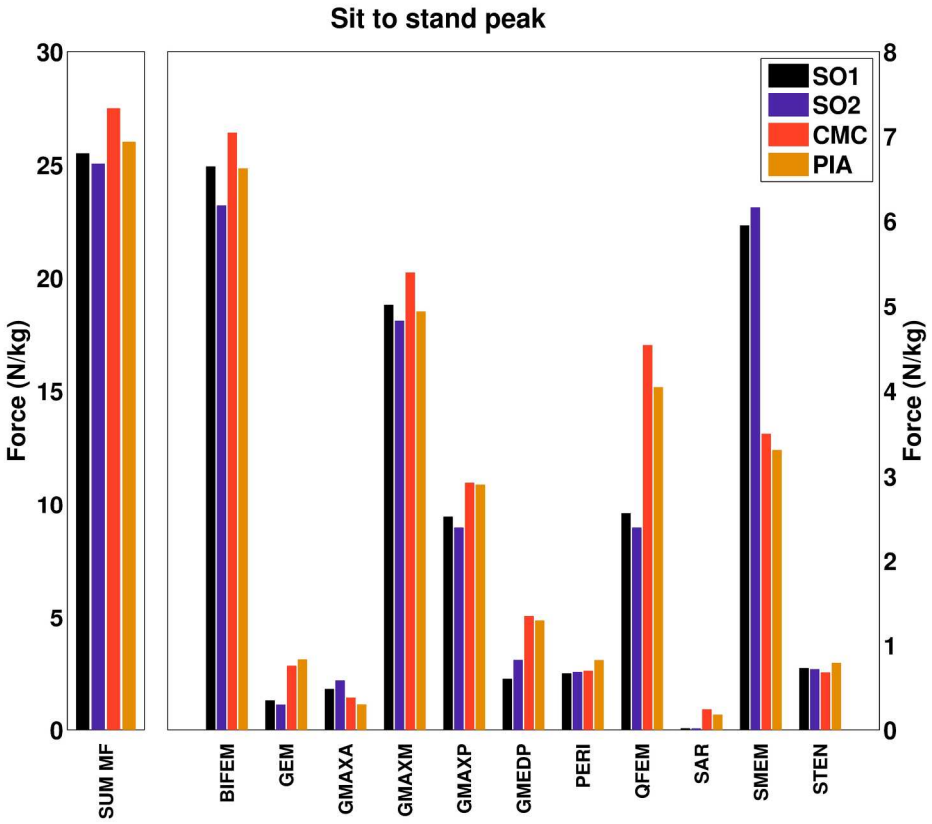

Figure 6V. Calculated muscle forces and sum of the muscle forces (SUM MF) for the different optimization techniques for the peak in sit to stand. The most active muscles spanning the hip joint are shown. The force delivered by other muscles is generally lower than 1N.
218x182mm (300 x 300 DPI)

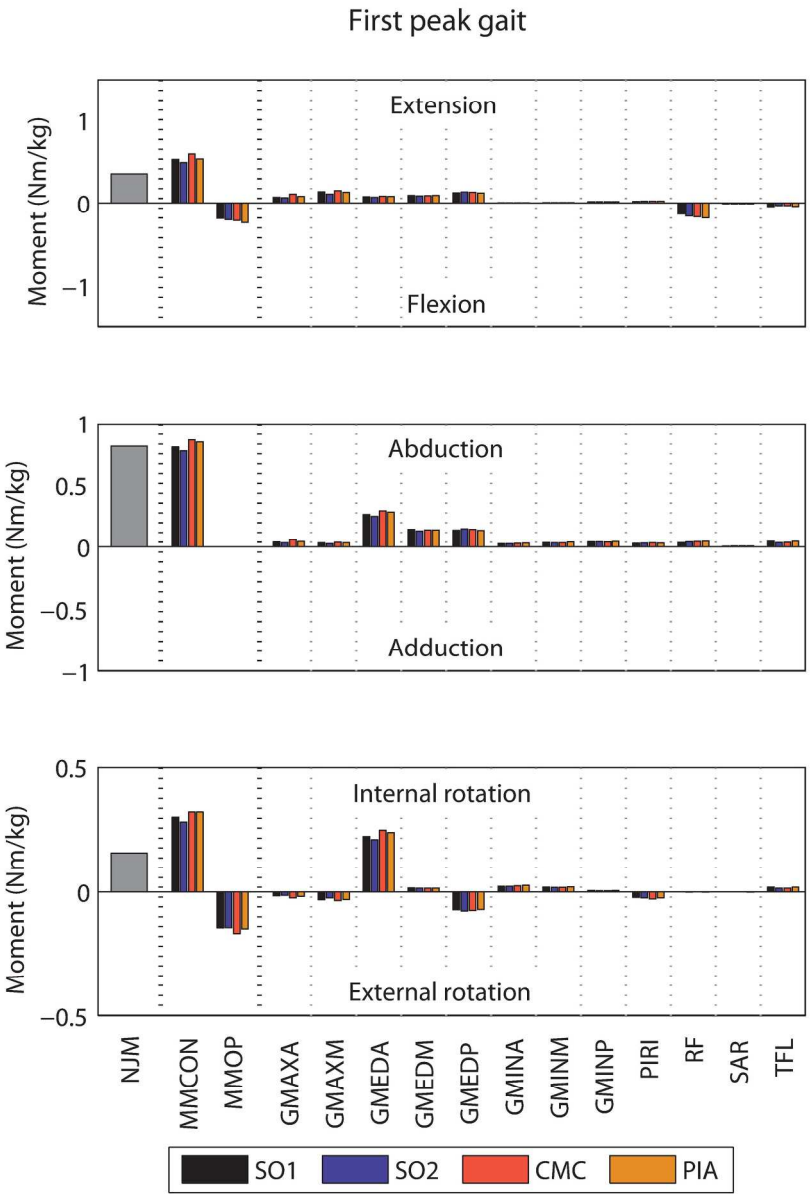

Figure 7A. Contribution of muscles to the hip moments at the first peak during gait. NJM is the net the joint moment calculated using an inverse dynamics procedure, MMCON and MMOP are respectively the sum of muscle moments contributing to and opposing the net joint moment. Note the different scales on the vertical axes.
193x254mm (300 x 300 DPI)

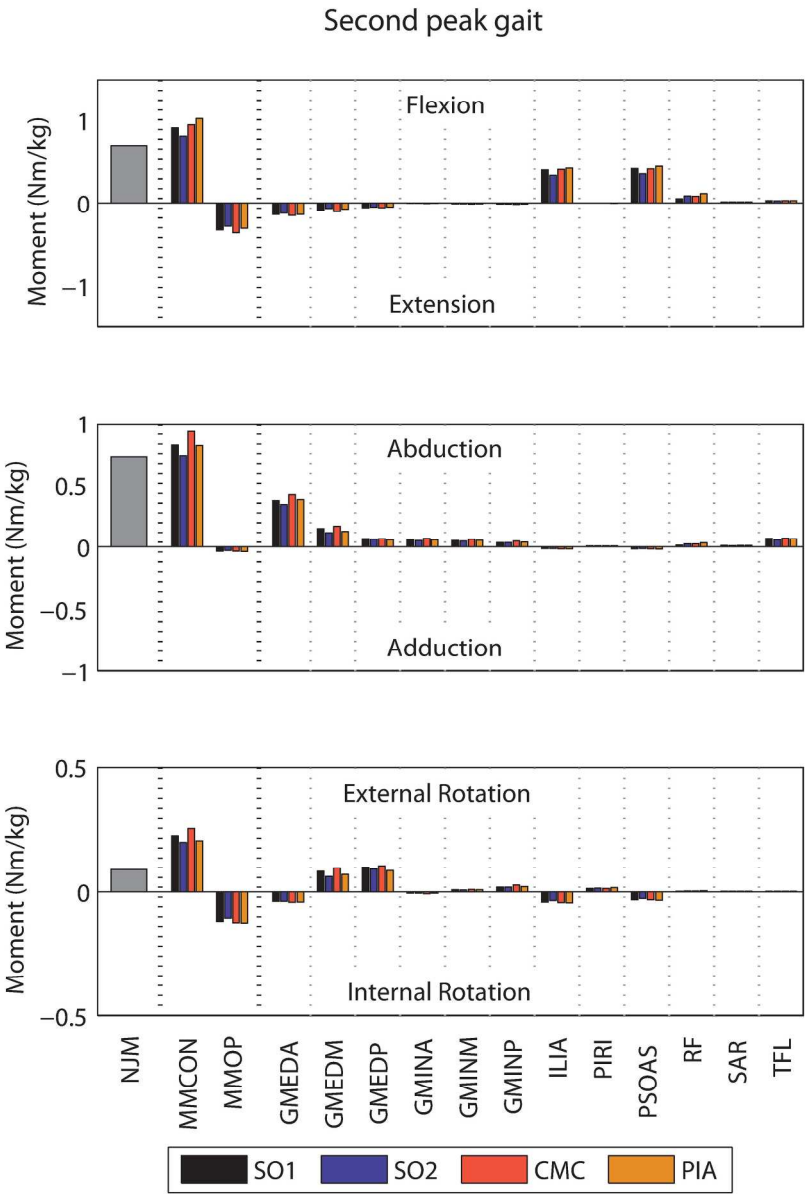

Figure 7B. Contribution of muscles to the hip moments at the second peak during gait. NJM is the net the joint moment calculated using an inverse dynamics procedure, MMCON and MMOP are respectively the sum of muscle moments contributing to and opposing the net joint moment. Note the different scales on the vertical axes.
193x254mm (300 x 300 DPI)

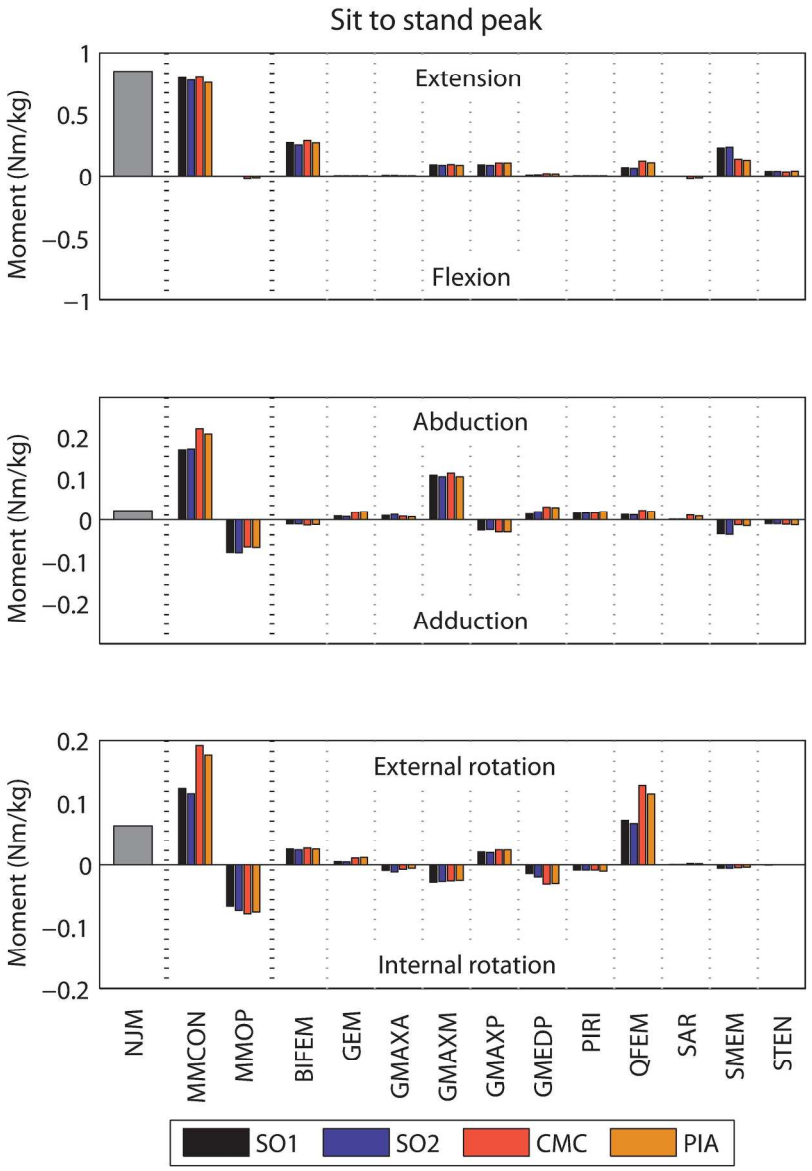

Figure 7C. Contribution of muscles to the hip moments at the peak in sit to stand. NJM is the net the joint moment calculated using an inverse dynamics procedure, MMCON and MMOP are respectively the sum of muscle moments contributing to and opposing the net joint moment. Note the different scales on the vertical axes.
193x254mm (300 x 300 DPI)

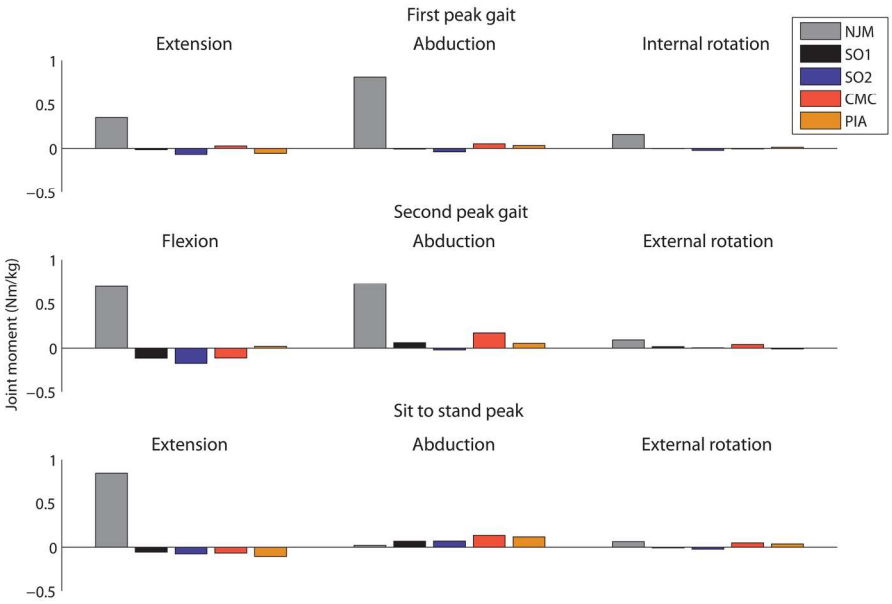

Figure 8. Net joint moment (NJM) and the difference between absolute muscle generated moment and net joint moment for the different optimization techniques, e.g. the deviation from the net joint moment. When the net joint moment is satisfied by the optimization, the muscle moment and joint moment will be equal, i.e. the difference between muscle moment and net joint moment is zero.
175x116mm (300 x 300 DPI)

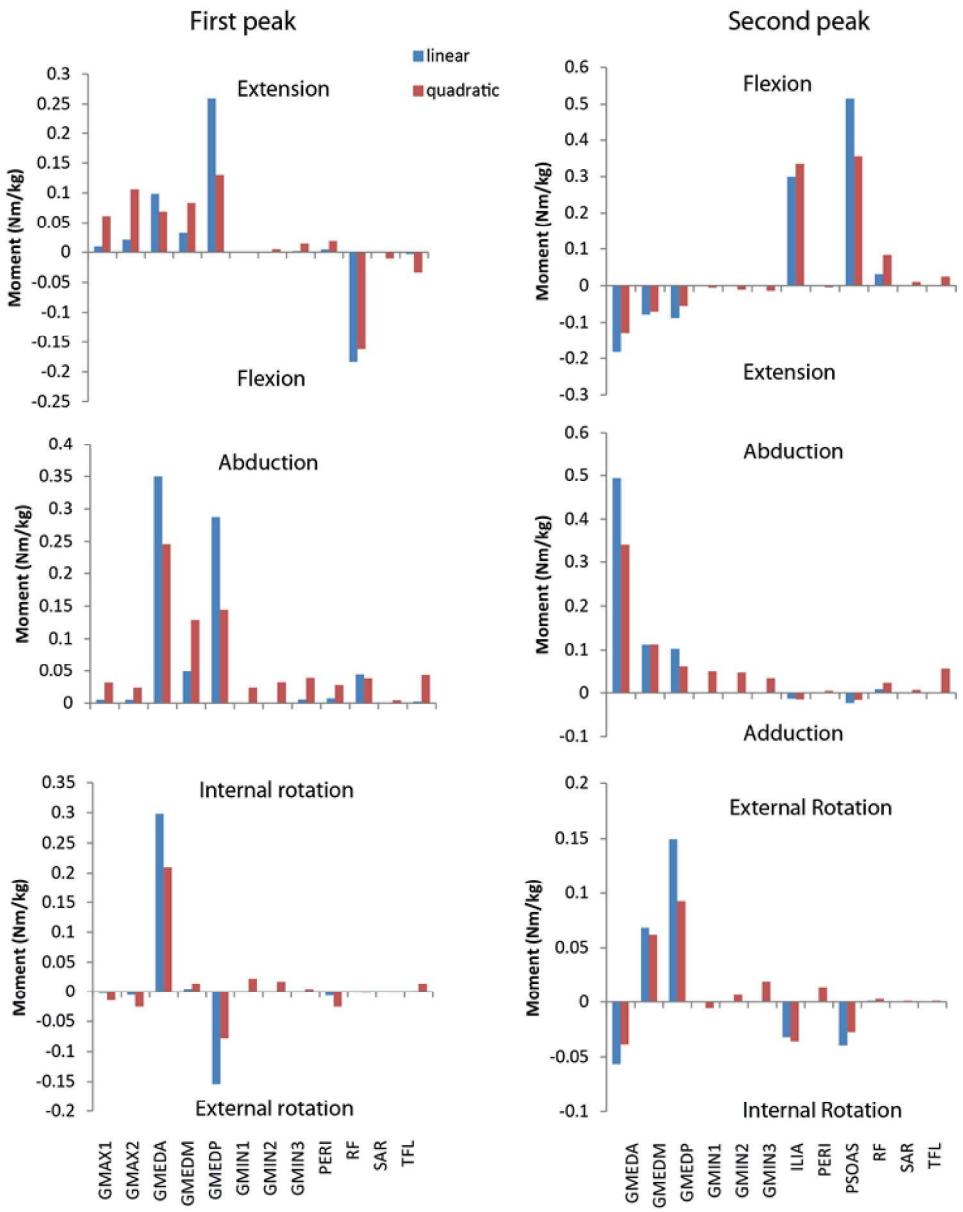

Review_Figure1. Contribution of muscles to the hip moments at the first (left) and second (right) peak during gait for SO2 using linear and quadratic optimization.
336x424mm (300 x 300 DPI)